WWW.IJRPR.COM

International Journal of Research Publication and Reviews

Journal homepage: www.ijrpr.com ISSN 2582-7421

Mantsaborivaky Milanoa Copper Mineralization, Vohemar District in the North-Eastern Part of Madagascar

Mirana Razoeliarimalala [a,b], Wu Datian [c,d], Wanming Yuan [c], Heninjara Narimihamina Rarivoarison [e], Luc Rabefihavanana [f], Rachel Razafimbelo [a]

[a] *Department of Earth Sciences and Environment, Faculty of Sciences and Technology, University of Antananarivo, Madagascar*
[b] *Doctoral school of Earth Sciences and Evolution, Faculty of Sciences and Technology, University of Antananarivo, Madagascar*
[c] *School of Earth Sciences and Resources, China University of Geosciences, Beijing 100083,China*
[d] *Nanjing Center, China Geological Survey, Nanjing 210016*
[e] *Department of Applied Geosciences, German University of Technology in Oman, Sultanate of Oman*
[f] *Department of Mathematics and Computer Science, Faculty of Sciences and Technology, University of Antananarivo, Madagascar*
DOI : https://doi.org/10.55248/gengpi.6.0225.0960

A B S T R A C T

Amongst 300 copper occurrences identified in the Vohémar district, the Mantsaborivaky Milanoa sector is the best known and has been exploited since 1915. This work focuses on petrographic studies and whole rock analysis of igneous and metaigneous rocks samples in order to clarify their magmatic and tectonic affinities, as well as their metallogenic implications as a guide for prospecting. Petrographically, the rocks reveal a past derived from ancient basic eruptive rocks, as well as retrograde metamorphism expressed mainly by epidotization accompanying the copper mineralization. Thus, these thin sections reveal important hydrothermal alteration dominantly propylitic, sericitic alterations and silicification. Thirteen samples were selected for analyzing major and trace elements using XRF, ICP-OES and ICPMS methods. Values of 48.34 wt %< SiO2 < 71.45 wt % and 0.5 wt % < K20< 15.91 wt % indicate calc-alkaline (moderate to potassium-rich) and tholeitic dominated magmatism. The variation in CaO and Al2O3 content in relation to SiO2, the silica and alkali enrichment in the residual liquid also confirm the fractional crystallization process of the same magma. The trace elements composition, showing enrichment in light rare earth elements (LREE) and Large Ion Lithophile Elements (LILE) compared to high field strength elements, indicate a subduction zone magmatism of subplate origin. It originates in an active continental margin and after partial melting of the lithospheric mantle. The negative europium anomalies, gently sloping rare earth spectra and moderate Sr values justify a volcanogenic sulphide cluster mineralization deposited in a Kuroko-type back-arc basin.

Keywords: Mantsaborivaky-Milanoa, calkalcalic magmatism, back arc basin, hydrothermal alteration, Kuroko type VMS

1. Introduction

Among the copper-bearing areas in Madagascar, Vohémar district is known for the ubiquity of copper occurrences in all geological formations (Jourde, G.,1968), especially the sector of Mantsaborivaky Milanoa. Previous studies have provided petrographic, lithostratigraphic, structural, geochemical, geochronological (BRENON, P., 1952 ; BRENON, P., 1954; BRENON, P.1956; La Roche, H.D., 1958; ; La Roche, H.D.1963; Jourde, G. et al.,1967; Jourde, G. et al., 1968 ; Bousteyak, L.,1974) and geodynamics datas (Tucker,R. et al., 1999 ; Collins et al.,2002 ; Jons et al.,2005 ; Thomas, R.J, et al., 2009 ; Tucker,R. et al., 2014) determining the origin, nature, character and age of the Bemarivo Domain and its position in the Gondwana supercontient. In summary, the calcoalcalic magmatism, the different metamorphic events especially the responsible for the strong epidotization, the different tectonic accidents acquired from the East African orogeny can demonstrate and explain the significant potentiality and ubiquity of the copper mineralization in Mantsaborivaky Milanoa (La Roche, H.D., 1958). Some of these studies have been carried out for a metallogenic and prospective aims, however the lack of precise and complete informations for identifying economically exploitable copper deposits limits their exploitation. On the one hand, Jourdes, G., et al., in 1968 concluded that the copper mineralization in the area is secondary and linked to the remobilization of this metal, and is considered as any significant economic interest. On the other hand, BRGM in 1985 suggested that the economic deposit has yet to be located.

In this paper, petrographic description and new geochemical datas obtained after whole rock analysis are presented and interpreted in order to understand the copper metallogeny as well as the type of copper deposit affiliation of the Mantsaborivaky Milanoa area in the Vohémar district.

2. Geological background

The study area, is located in the north-eastern part of Madagascar in the Northern Bemarivo Domain or Bobakindro Domain (Armistead, et al., 2019). It is separated from the Southern Bemarivo Domain or Marojejy Domain by the east-west trending Antsaba shear zone dated 720 Ma (Thomas, R.J. et al.,2009). Two metavolcano-sedimentary formations and two plutonic formations, which are calc-alkalic to tholeitic affinities have been recognized by field research and U–Pb SHRIMP ages from the U–Pb zircon geochronology (Thomas,R.J. et al.,2009 ; Tucker,R. et al.,2014).

These metavolcano-sedimentary formations are composed by: the Milanoa Group formed by metavolcano-sedimentary rocks dated from 750Ma resulted from a metamorphism under amphibolite facies and the Daraina Group made up of volcanic and vocanoclastic rocks dated from 720Ma to 740 Ma and metamorphosed under the greenschist to amphibolite facies. Strong migmatization of the old mafic eruptive rocks is common in zones of higher metamorphic intensity from the base to the top of the amphibolite facies (Jourdes, G., 1968; Bousteyak, L., 1974). The two plutonic formations observed in the study area are the Manambato Suite and the Maevarano Suite. Together with the Betsiaka Group, which is outside of our study area, the two metavolcano-sedimentary formations have been intruded by a large calc-alkaline plutonic complex, the Manambato Suite between 705 and 718 Ma, and the late granite Maevarano Suite (520Ma - 540Ma), which was emplaced just at the end of the Gondwana amalgamation (Thomas, R.J. et al.,2009). It is characterised by the absence of prograde metamorphism and a few traces of retromorphism (BGS, 2008). The Antsirabe Nord suite, also calc-alkaline separating the two domains, is not included in our study area.

The study area exhibits submeridional foliation trajectories. Two main directions of brittles structures WNW- ESE and NNE-SSW were recognized. They are acquired during the East African orogeny between 520 and 540 Ma and the post-collisional extension of the Cretaceous (Bousteyak, L., 1974; BGS,2008; Razoeliarimalala, M.,2013). More than 300 copper occurrences have been recorded (CEA, 1980), as Mantsaborivaky Milanoa copper mineralization in the orthoamphibolitized dolerites which had exploited since 1915. According to La Roche, H.D., 1954, the copper ores are disseminated in quartz veins or concentrated as impregnation in the dolerites or amphibolite gneisses near the contacts. It mainly consists of chalcopyrite, then becomes unstable and is replaced by bornite, the primary copper ore. However, bornite is replaced by chalcocite as a result of enrichment in the cementation zone and Malachite, azurite, bronchantite, chessylite are products of surface alterations (La Roche, H.D., 1954).

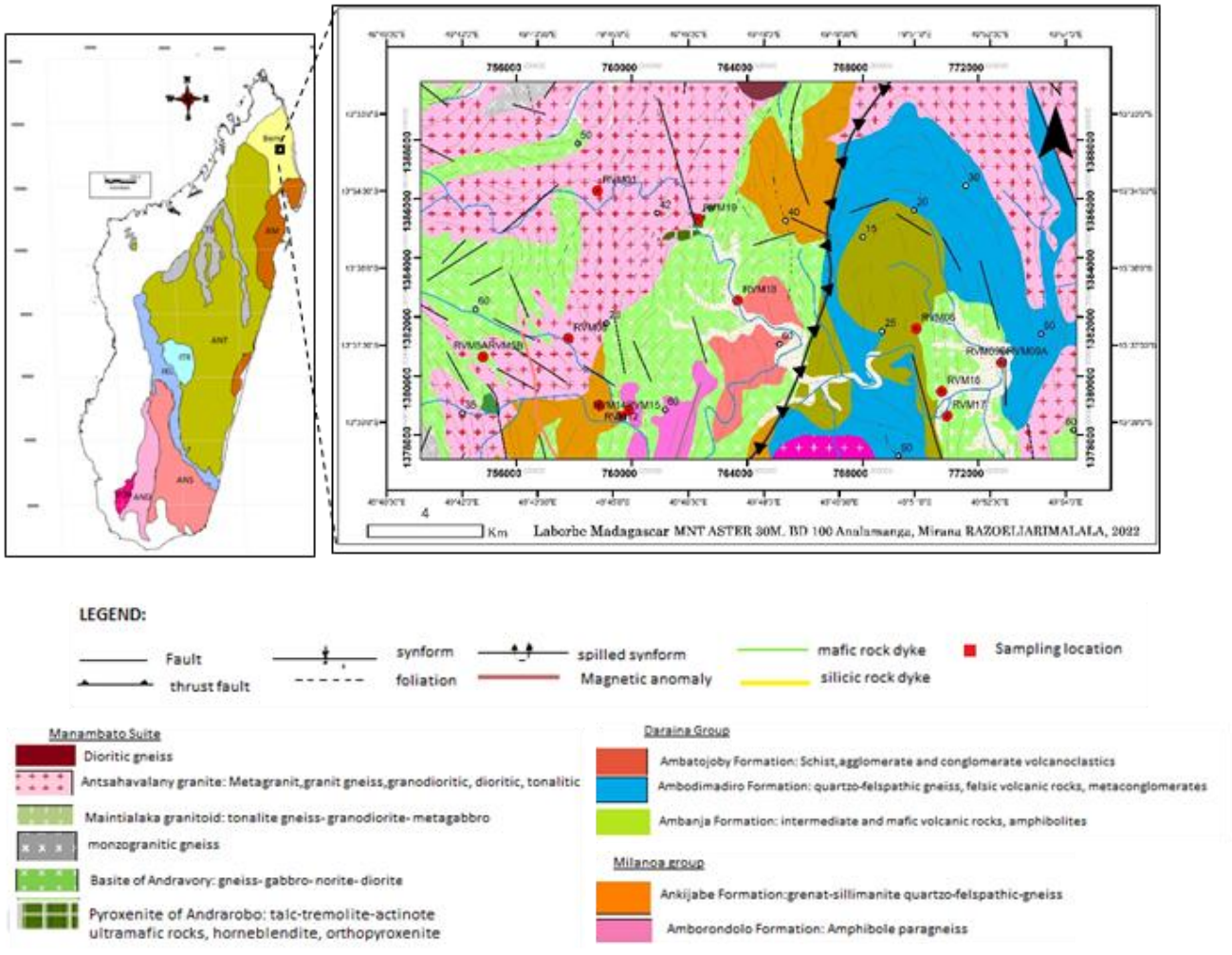

Fig. 1: geological map of Mantsaborivaky Milanoa area modified after Roig et al. 2012; Bem= Bemarivo Domain, AM= Antongil Masora Domain, ANT= Antananarivo domain, TS= Tsaratanana complex, ITR= Itremo group

3. Analytic methods

In this research, thirteen representative samples from Mantsaborivaky Milanoa sector were selected for petrographic studies of thin sections prepared at the Georesources and Environment Laboratory of the Earth and Environmental Sciences Department at the Antananarivo University. These same samples were cleaned and stripped of weathered parts before pulverization with a grain size of -0.8 mm (20 mesh) for major and trace elements analysis (Table 1). All analysis were carried out at the Northeast Mineral Resources Supervision and Testing Center of Land and Resources in Shenyang and at the Tianjin Center, China Geological Survey.

Major elements were obtained using the X-ray fluorescence method on a ZSX Primus- Rigaku and the ICP-OES method on an American iCAP6300 Radial direct-reading thermoelectric full-spectrum inductively coupled plasma spectrometer. The detection limit ranges from 0002 to 0.06%.

Loss on ignition (LOI) were obtained after weighing 0.5g of powder samples burnt at 1000°C for one hour. After mineralization of 0.25 g of powder sample with 25ml of HF-HCl-HNO3-HClO4-H2SO4 aqua regia followed by dilution, the solution was analysed by ICP-MS on the XSERIES 2 thermoelectric inductively coupled plasma mass spectrometer for trace elements. Other elements are determined on the Rigaku ZSX Primus fluorescence spectrometer. The detection limit is 0.27 to 8 parts per million (ppm). Analysis and quality testing of samples are carried out in accordance with the requirements of DZ/T 0258-2014 Multi-target Area Geochemical Survey Specification (1:250000) and DZ/T 0130 Geological and Mineral Testing Quality Management Specification.

4. Results

4-1 Petrography

The thirteen rocks samples are presented in Table 1 with their respective locations and natures. After observations in optical microscope, the rocks collected are defined as follows:

Table 1: Sampling location and the main geological formation in Mantsaborivaky Milanoa area

	Location		**Suite/Group**
RVM 01	S13° 34’ 12’’	E49° 45’ 04,8’’	Manambato suite
RVM 05 A and RVM05 B	S13° 37’ 37,33’’	E49° 42’ 55,74’’	Manambato suite
RVM 06	S13° 37’ 12’’	E49° 44’ 33,72’’	Manambato suite
RVM 08	S13° 36’ 36’’	E49° 51’ 14,10’’	Daraina group
RVM 09A	S13° 37’ 12’’	E49° 52’ 53,28’’	Daraina group
RVM 12	S13° 38’ 24’’	E49°45 ‘ 10,44’’	Milanoa group
RVM 13	S13° 38' 24"	E49° 45' 44,64"	Milanoa group
RVM 14	S13° 38’ 34,8’’	E49° 45’ 35,88’’	Milanoa group
RVM16	S13° 38’ 2,4’’	E49° 51’ 44,64’’	Daraina group
RVM17	S13° 38' 31,2"	E49° 51' 51,30"	Manambato suite
RVM18	S13° 36' 25,2"	E49° 47' 4,80"	Manambato suite
RVM19	S13° 34' 58,8"	E49° 47' 0,60"	Manambato suit

Granodioritic gneisses: RVM01 -RVM05A are bluish-white rocks speckled black, medium to coarse grains. They show granoblastic textures made up of quartz, perthitic orthoclase, microclines, myrmeckite, oligoclase-type plagioclase with saussuritized and cataclastic andesine. Feldspars with inclusions of small crystals including sillimanite. The green hornblende and other amphiboles transformed into a mineralogical association such as: epidote (Pistachite) + chlorite+ actinote+ quartz. Brown to greenish-brown biotite, epidote and granular sphene Opaque magnetite crystals, Pyroxene relics were also observed. (Razoeliarimalala, M., 2013) (Fig. 2a -2b)

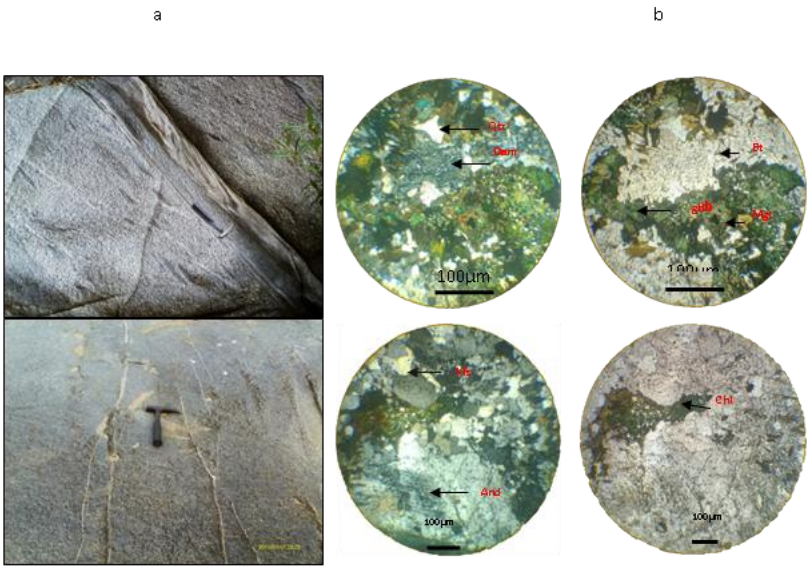

Fig. 2: (a) granodioritic gneisses outcrops of RVM01 showing amphibolites xenoliths and RVM 05A; (b) Photomicrograph showing the representative rock texture and main mineral assemblage (in the left under cross polarized light, in the right under plane polarized light). Mineral abbreviations: Qtz = quartz; Kfs = K-feldspar; And= andesine; Bt = biotite; Chl= chlorite, gHb = green Hornblende; Dam= damourite; Mgt= magnetite.

Orthogneiss: RVM 5B shows minerals with an almost homogeneous grain size. The modal composition shows a balanced content between light minerals (quartz and feldspars) and dark minerals (biotite + pyroxene + amphibole), brown hornblendes of damouritization and kaolinization are observed, respectively, in the plagioclases and potassium feldspars. (Fig. 3)

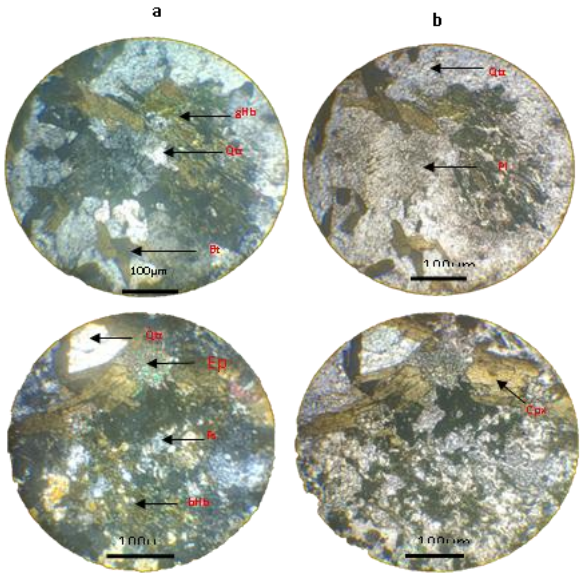

Fig. 3.: typical photomicrograph showing the representative rock texture and main mineral assemblage of the orthogneiss sample RVM05B (a) under cross polarized light, (b) plane polarized light). Mineral abbreviations: Qtz = quartz; Fs == feldspar; Pl= plagioclase; Bt = biotite; gHb = green Hornblende; bHb= brown hornblende; Cpx= clinopyroxene

Quartzo -felspathic gneiss: RVM12 is greyish-white to pinkish in colour, fine to medium-grained with a heterogranular granuloblastic structure. It is composed of flattened quartz that is often jagged and interlocked, oligoclase, orthoclase, large microcline, numerous greenish-brown biotites and numerous opaque granular minerals. (Fig. 4a -4b)

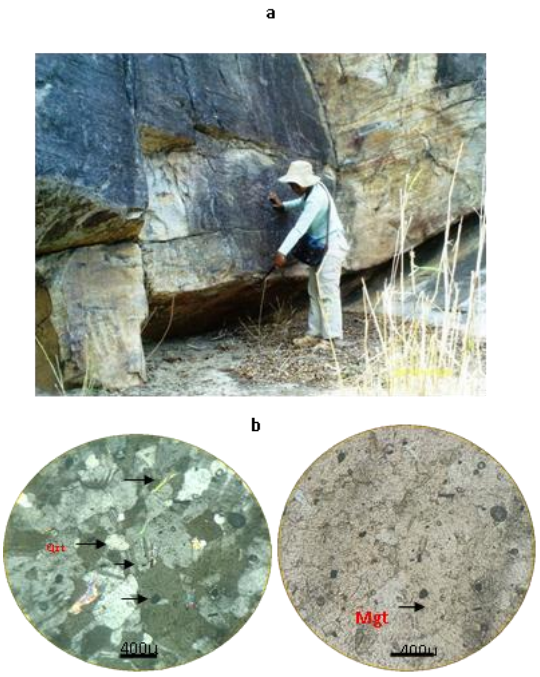

Fig. 4: (a) quartzo-fedspathic gneiss outcrops of RVM12; (b) Typical photomicrograph showing the representative rock texture and main mineral assemblage (in the left under cross polarized light, in the right plane polarized light). Mineral abbreviations: Qtz = quartz; Bt = biotite; Olg= oligoclase; Mgt= magnetite.

Gabbro: RVM09A - RVM 19 are dominated by basic minerals: pyroxene and basic plagioclase with a nematoblastic structure. They consist of damouritized and sericitized orthoclase, xenomorphic magnetite developed in intercrystalline microfractures or on the altered pyroxene, biotite, green hornblende, relics of some residual augite and diopside, chlorite, traces of apatite, zircon and epidote (Jourde, G., 1968; Razoeliarimalala, M., 2013) (Fig. 5).

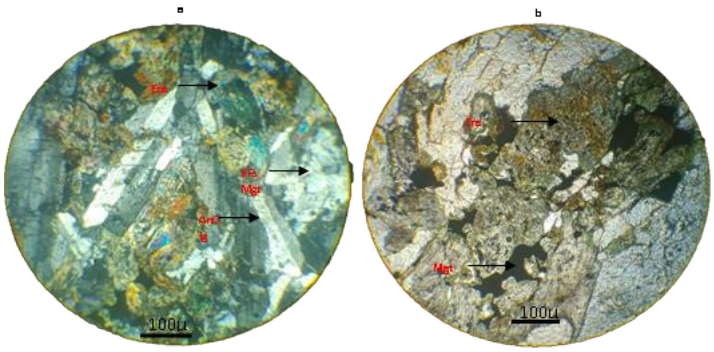

Fig.5: typical photomicrograph showing the representative rock texture and main mineral assemblage of the sample RVM09A (a) under cross polarized light, (b) plane polarized light. Mineral abbreviations: Qtz = quartz; And= anorthite; K feldspar; Bt = biotite; Ens= enstatite; Mgt= magnetite

Amphibolites: RVM 06 - RVM08- RVM13 are dark blue-grey to bluish, sometimes turning green when the epidote is fairly abundant or black (BRENON, P., 1952). They cover a fairly large area in the study area, sometimes appearing as clasts in schistose matrices or as enclaves in granodioritic gneisses. They show a granulolepidonematoblastic structure, a transformation of the amphibole into a mineralogical association such as: epidote (pistachite) + chlorite + actinote + quartz, as well as significant sericitisation and damouritisation. (Razoeliarimalala, M., 2013).

RVM 13 shows the presence of acicular sillimanite, inclusions of small prismatic Apatite crystals in feldspar and amphibole beds (Razoeliarimalala, M., 2013)

RVM 08 shows quartzo-feldspathic veins that are consistent with foliation and the transformation of ferromagnesian minerals into an association of Biotite + Hornblende + Chlorite + Quartz + opaque minerals (Razoeliarimalala, M., 2013) (Fig. 6a -6b)

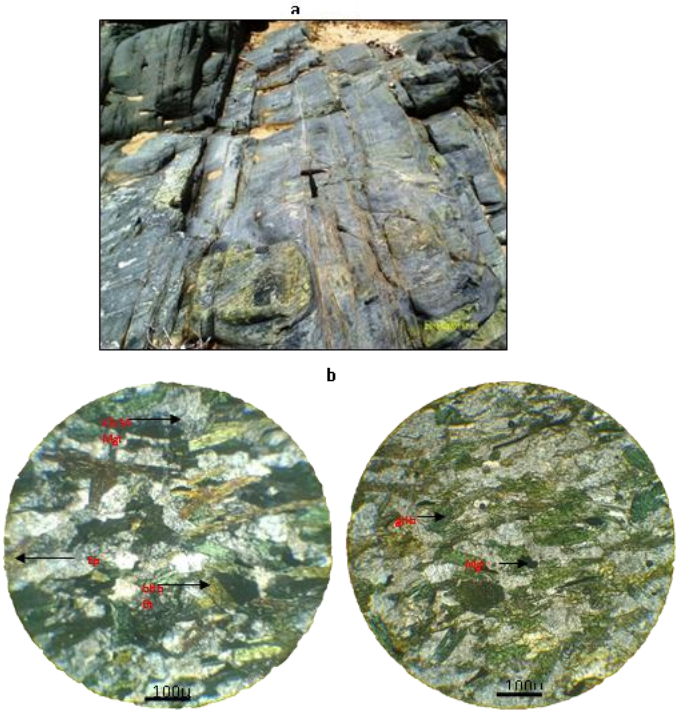

Fig.6 :(a) epidotized amphibolite outcrops of RVM08; (b) Typical photomicrograph showing the representative rock texture and main mineral assemblage (in the left under cross polarized light, in the right plane polarized light). Mineral abbreviations: KFs = potassic feldspar; gHb = green hornblende; bHb= brown hornblende; Mgt=magnetite

Dolerite: RVM 14 is a fine-grained, bluish-grey rock with a gritty, ophitic structure and granoblastic recrystallization with green hornblendes, amphibole transformed into a mineralogical association such as epidote (pistachite) + chlorite + actinote + quartz, pyroxene relics, biotite, saussuritized and cataclastic andesine, little pyroxene relics, and andesine relics: epidote (pistachite) + chlorite+ actinote+ quartz, relics of pyroxene, biotite, saussuritized and cataclastic andesine, little granoblastic quartz, little apatite, magnetites in granular form at the edge of the amphibole, numerous hematites, Sphene in inclusion in the amphibole have been highlighted (Razoeliarimalala, M., 2013) (Fig. 7)

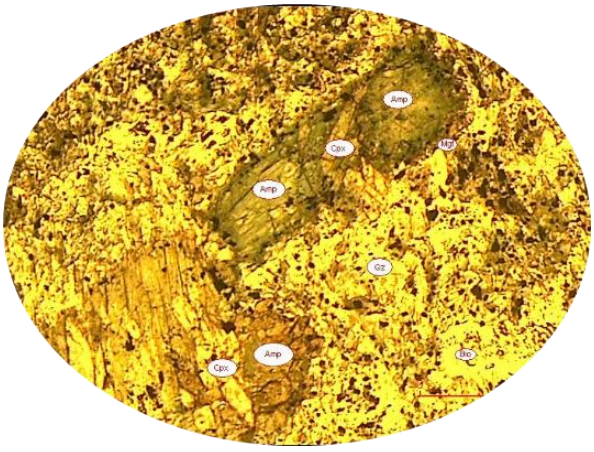

Fig. 7: typical photomicrograph showing the representative rock texture and main mineral assemblage of the sample RVM14 under cross polarized light showing the transformation of ferromagnesian minerals to the association of Qz+Chl+ opq+Amp and the concen concentration of Magnétite around the amphibole. Mineral abbreviations: Amp= amphibole; Cpx= clinopyroxene; Bio = biotite; Qz= quartz; Mgt=magnetite; op= opaque minerals

Metadiorite: RVM18 is a greenish or blackish grey rock with a heterogranular granuloblastic structure and consists of oligoclase and andesine, hornblende, greenish-brown biotite, quartz, potassium felspar, apatite and opaque minerals (Razoeliarimalala M., 2013)

4-2. Whole rock geochemistry

The geochemical results are illustrated in Table 2, except for the elements Be, U and Ta, which are all below the detection limit.

Table 2: Whole-rock elemental data for samples from Mantsaborivaky Milanoa area

Samples n°	RVM01	RVM05A	RVM05B	RVM06	RVM08	RVM09A	RVM12	RVM13	RVM14	RVM16	RVM17	RVM18	RVM19
Major elements (wt%)													
SiO_2	60,90	61,07	71,45	52,58	48,34	48,72	73,00	52,01	59,10	53,69	56,68	58,37	53,12
Na_2O	4,21	4,62	4,00	3,18	2,71	4,33	3,61	4,11	2,68	2,28	3,86	2,68	3,28
MgO	2,36	2,14	0,28	8,46	7,05	4,71	0,30	4,53	3,65	8,24	3,78	5,93	6,23
Al_2O_3	17,03	18,30	15,85	14,06	16,82	19,37	14,00	19,41	15,93	13,57	17,80	14,38	17,27
P_2O_5	0,24	0,18	0,043	0,21	0,086	0,52	0,047	0,30	0,19	0,17	0,25	0,21	0,20
K_2O	3,33	2,71	3,42	1,79	1,36	0,95	5,91	1,36	0,51	0,59	2,30	0,72	1,07
CaO	4,64	5,06	2,72	8,72	10,77	8,79	0,48	7,74	9,00	11,78	6,63	8,72	9,80
TiO_2	0,86	0,58	0,16	0,66	1,07	1,67	0,33	1,00	0,76	0,84	0,90	0,57	0,64
MnO	0,10	0,076	0,017	0,15	0,17	0,17	0,041	0,14	0,11	0,25	0,12	0,12	0,12
Fe_2O_3	2,41	2,22	0,89	7,07	6,47	4,16	1,52	3,60	3,83	3,24	2,98	3,81	3,01
FeO	3,17	2,16	0,50	1,51	3,59	6,28	0,17	4,39	3,22	4,25	4,17	3,31	3,72
LOI	1,06	1,04	0,74	1,76	1,90	1,02	0,52	1,82	1,37	1,51	0,96	1,54	1,88
TOTAL	100,3094	100,1648	100,0569	100,15009	100,32761	100,6823	99,944	100,42259	100,35276	100,426	100,4145	100,3513	100,3356
Trace elements (ppm)													
Ba	*0.10	*0.12	*0.21	608	315	*0.14	*0.18	586	427	451	795	552	279
Cr	21,5	18,3	8,34	457	206	33,8	7,32	44,5	136	393	58,3	329	132
Cu	63,4	38,6	40,4	76,1	446	93,6	24,1	106	361	9,87	730	24,1	33,9
Ga	21,7	21,3	16,3	17,2	18,9	25,8	21,9	22,8	19,7	19,8	20,8	19,4	19,0
Nb	12,8	7,16	4,00	6,08	5,98	9,80	17,3	5,67	12,9	8,83	6,34	5,53	5,17
Ni	11,0	13,1	0,96	139	57,4	13,5	1,11	22,4	40,0	64,1	18,9	121	67,3
Pb	21,9	21,5	27,8	9,03	5,91	11,8	32,6	10,8	12,0	6,17	12,9	9,48	10,4

Rb	86,2	57,6	52,6	45,0	22,6	8,11	132	28,3	5,55	2,52	59,2	13,8	28,8
Sr	543	780	834	543	359	780	99,6	716	894	547	611	780	647
V	94,7	74,6	20,4	156	198	213	16,8	154	142	158	133	137	133
Zn	71,3	57,6	21,3	75,7	82,7	113	108	94,9	61,4	104	76,4	64,6	63,8
Li	17,4	13,1	5,16	7,85	5,77	7,28	12,8	9,37	5,68	2,37*	14,1	5,24	8,87
Sc	16,2	10,8	1,69*	32,8	35,5	31,3	10,5	22,4	19,9	61,1	19,9	22,1	31,9
Co	15,7	12,3	2,45*	28,7	31,9	30,4	3,14*	23,2	19,4	23,8	20,7	22,0	23,8
Th	11,9	4,76	6,26	4,90	2,54*	3,98*	8,72	4,91	5,77	5,87	6,82	5,38	4,76
Hf	7,60	3,44	3,40	2,89	1,71	6,69	12,6	2,88	3,65	2,51	4,27	3,16	2,51
Cs	2,56	1,61	0,75	0,49	0,64	0,17	2,72	1,19	0,20	0,10	2,08	0,15	0,48
Tl	0,23	0,15	0,11	0,13	0,040	0,021*	0,42	0,085	0,016*	0,0010*	0,19	0,028	0,084
Y	26,3	12,8	5,19	17,1	18,7	31,1	61,5	20,6	14,8	26,9	20,7	12,0	13,5
La	36,3	23,7	17,5	14,0	6,81	30,2	60,5	21,9	18,9	27,4	26,7	15,2	14,0
Ce	69,8	45,5	33,7	28,2	11,7	57,3	110	41,7	35,5	62,4	49,4	27,0	27,7
Pr	9,95	5,85	3,61	4,64	2,77	9,89	17,3	6,65	5,37	10,2	7,15	3,86	4,41
Nd	36,6	23,4	12,7	19,6	15,0	45,4	65,9	27,8	26,1	41,5	29,3	22,2	20,5
Sm	8,06	4,47	1,86	4,80	3,69	10,2	14,9	6,06	4,60	8,91	6,10	3,51	3,86
Eu	1,87	1,46	1,10	1,53	1,43	2,93	3,48	2,02	1,33	2,33	1,83	1,16	1,17
Gd	6,81	3,74	1,59	4,65	4,20	9,04	13,2	5,59	4,41	8,50	6,08	3,61	3,94
Tb	0,77	0,40	0,14	0,55	0,58	1,04	1,64	0,63	0,49	0,94	0,70	0,41	0,47
Dy	4,69	2,34	0,83	3,38	3,64	6,15	10,2	3,88	2,90	5,66	4,18	2,48	2,74
Ho	0,90	0,43	0,16	0,65	0,73	1,16	2,01	0,74	0,56	1,07	0,81	0,48	0,52
Er	2,70	1,29	0,54	1,91	2,13	3,35	6,17	2,20	1,65	3,19	2,39	1,40	1,52
Tm	0,36	0,17	0,078	0,25	0,28	0,42	0,85	0,29	0,22	0,42	0,32	0,18	0,20

Yb	2,37	1,11	0,57	1,63	1,79	2,68	5,57	1,90	1,41	2,77	2,10	1,22	1,28
Lu	0,35	0,17	0,10	0,24	0,27	0,39	0,82	0,28	0,21	0,42	0,31	0,18	0,19
Eu/Eu*	1,12	0,92	1	0,93	0,76	1,06	0,9	0,97	0,82	0,77	1,09	1,96	0,99
LaN/SmN	1,16	2,76	2,72	1,86	2,55	2,28	2,58	0,93	1,93	2,83	3,33	5,91	1,83
LaN/YbN	2,57	8,58	8,58	7,6	7,32	7,77	8,99	3,41	6,66	10,32	14,34	20,85	5,77

***Under the detection limit**

- **Major elements**

As specified by the classification of Cox et al. (1979) adapted by Wilson (1989), the plutonic rock samples have a SiO_2 composition varying from 48.72 wt % to 76.55 wt % and a high total alkaline content ($Na_2O + K_2O$) from 3.4 wt % to 9.52 wt % with K_2O/Na_2O ratios varying from 0.26 to 1.89. They are enriched in Al_2O_3 ranging from 14% to 19.37%. According to the chemical classification and nomenclature of plutonic rock, they all belong to the tholeitic domain except for sample RVM 09A. They have a granitic to gabbroic composition and are therefore felsic to mafic (Fig. 8a).

The volcanic samples exhibit an SiO_2 composition ranging from 48.34 wt% to 59.10 wt%, with a high total alkali content ($Na_2O + K_2O$) between 2.87 wt% and 5.47 wt%, and K_2O/Na_2O ratios varying from 0.19 to 0.56. They are enriched in Al_2O_3, ranging from 13.47% to 19.41%, and, like the plutonites, are all situated within the tholeiitic domain. Their composition varies from andesitic to basaltic, classifying them as intermediate to mafic in nature (Fig.8b).

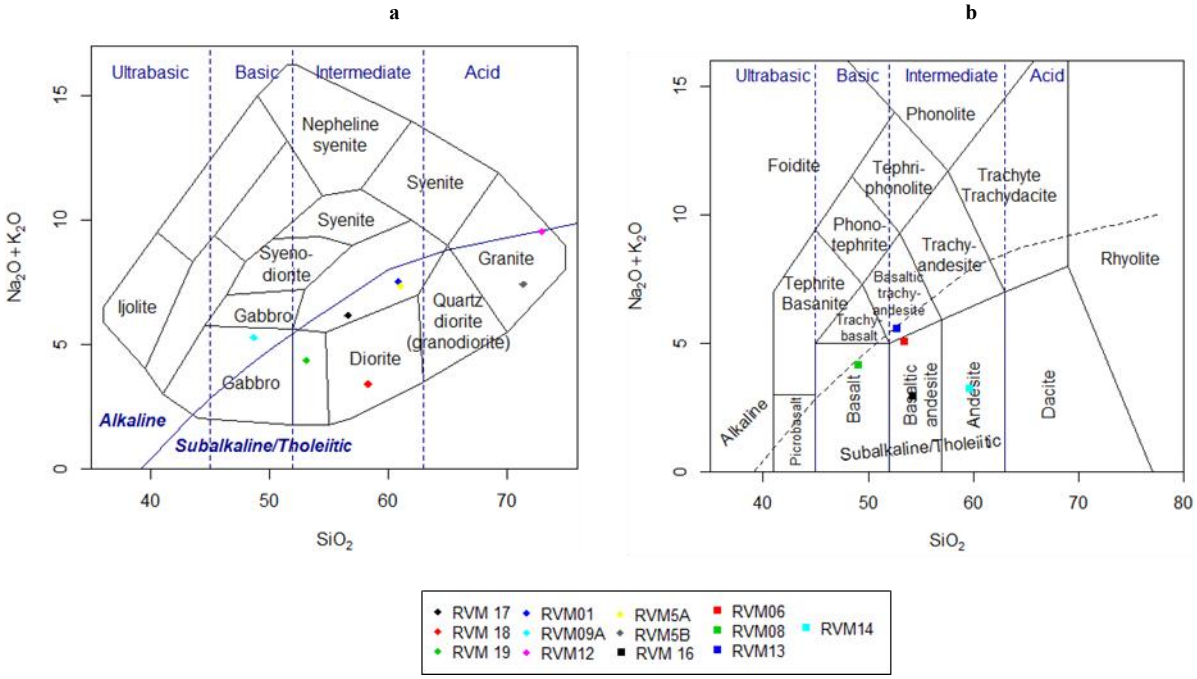

Fig. 8: (a) Chemical classification and nomenclature of plutonic rocks using the Total alkalis versus Silica diagram of Cox et al. (1979) adapted by Wilson (1989); (b) Chemical classification and nomenclature of volcanic rocks using the Total alkalis versus Silica diagram after Le Bas et al. (1979)

In the K2O Vs SiO2 diagram by Pecerillo and Taylor (1976), the magmatisms are calc-alkaline (moderately potassic and richly potassic) and tholeitic in nature, except RVM12, which is shoshonitic. (Fig. 9a).

According to Shand's (1943) index, with A/NK (Al_2O_3/ ($Na_2O + K_2O$) values ranging from 1.2 to 2.4 and A/CNK (Al_2O_3/ ($CaO + Na_2O + K_2O$) values between 0.8 and 1.12, all samples are metaaluminous. An A/CNK ratio below 1.1

The figure 10 illustrates the geochemical relationships between silica (SiO_2) and various oxides: MgO, CaO, TiO_2, and P_2O_5, exhibit moderate negative correlations with SiO_2, while FeO total shows a strong negative correlation. K_2O displays a moderate positive correlation with SiO_2, whereas Na_2O shows a weak correlation. Al_2O_3 initially correlates positively with SiO_2 before transitioning to a negative correlation. It also shows the observed depletion of P_2O_5, MgO, CaO, and TiO_2, alongside a progressive increase in SiO_2. Additionally, the Loss on Ignition (LOI) values of the metavolcanic samples in the study area range from 1.37 to 1.90 wt%.

The figure 11 illustrates a Harker diagram that highlights the geochemical behavior of copper (Cu) in relation to major oxides and trace elements. On one hand, Cu exhibits positive correlations with oxides such as CaO, Al_2O_3, FeO (total), MnO, TiO_2, MgO, and P_2O_5, as well as with trace elements including cobalt (Co), vanadium (V), lithium (Li), and zinc (Zn). On the other hand, Cu shows negative correlations with oxides such as SiO_2, Na_2O, and K_2O, as well as with trace elements like lead (Pb), nickel (Ni), chromium (Cr), rubidium (Rb), cerium (Ce), and lanthanum (La)

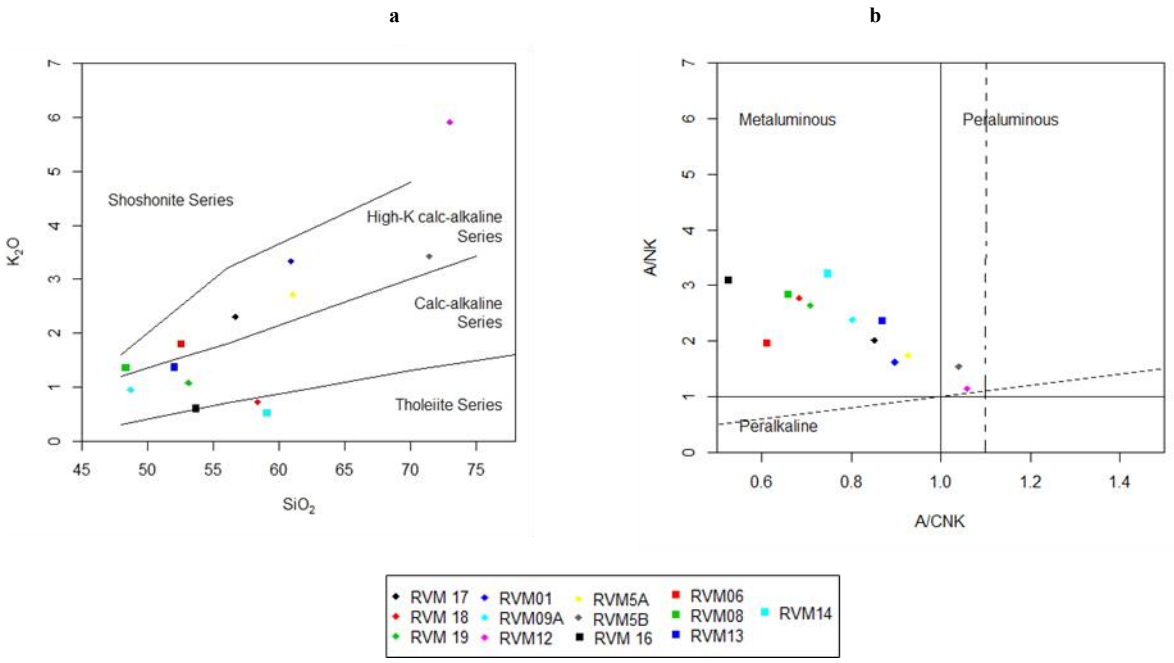

Fig. 9: (a) SiO_2 Vs K_2O diagram illustrating magmatic series, Pecerillo and Taylor (1976); (b) A/CNK - A/NK Diagram of plutonic rocks of the study area (Shand 1943)

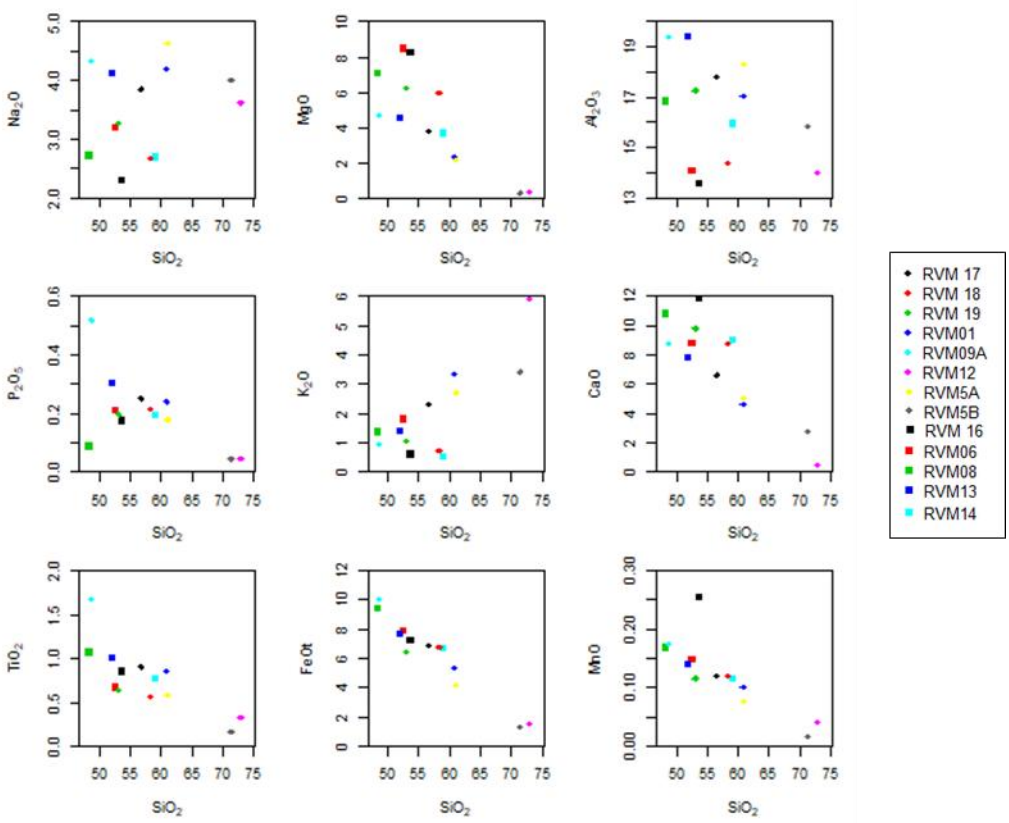

Fig.10: Harker variation diagrams of the representative samples of the study area between Silica with Na_2O-MgO-Al_2O_3-P_2O_5-K_2O-CaO-TiO_2-FeOt-MnO

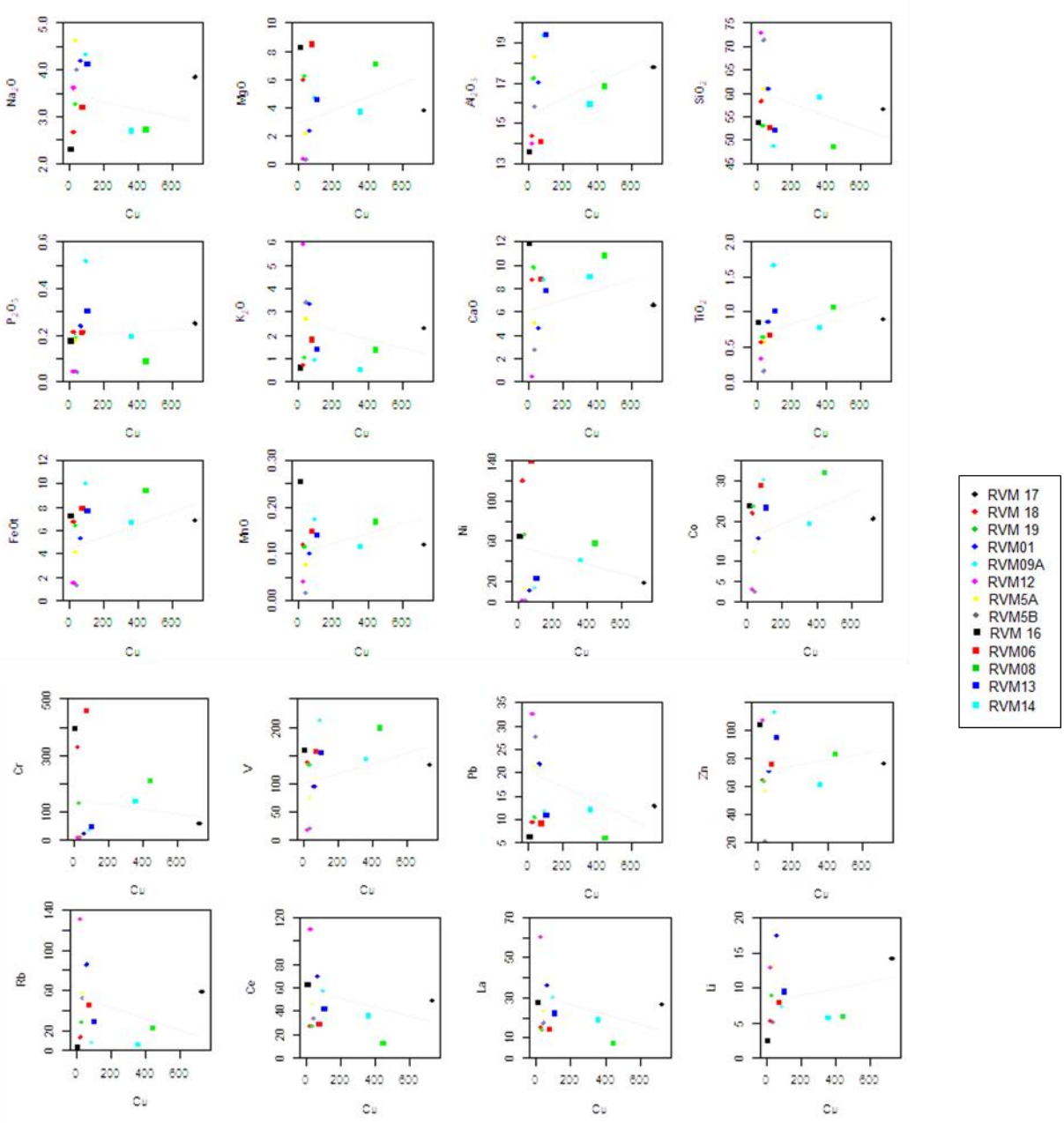

Fig. 11: Harker variation diagrams showing the relationships between copper (Cu) and major oxides and trace elements in representative samples from the study area.

Rare earth elements (REE):

The REE multi-element diagram is normalized to the primitive mantle following Sun and McDonough (1995) (Fig.12). The analyzed samples exhibit overlapping geochemical profiles, characterized by enrichment in Large Ion Lithophile Elements (LILE) relative to High Field Strength Elements (HFSE). Specific samples, such as RVM01, RVM12, RVM13, and RVM17, show significant enrichment in barium (Ba), while RVM06, RVM08, RVM13, RVM17, and RVM18 are notably enriched in cesium (Cs). Thorium (Th) enrichment is observed in nearly all felsic rock samples, with RVM09A displaying a remarkable enrichment in potassium (K) and lead (Pb). All samples exhibit pronounced negative anomalies in phosphorus (P), niobium (Nb), and titanium (Ti), indicating a relative depletion in HFSE elements such as Nb and Ti compared to other REEs. Additionally, LILE such as strontium (Sr), rubidium (Rb), and barium (Ba) show positive correlations with silica (SiO_2) (Fig. 13), suggesting their strong association with felsic minerals, particularly plagioclase.

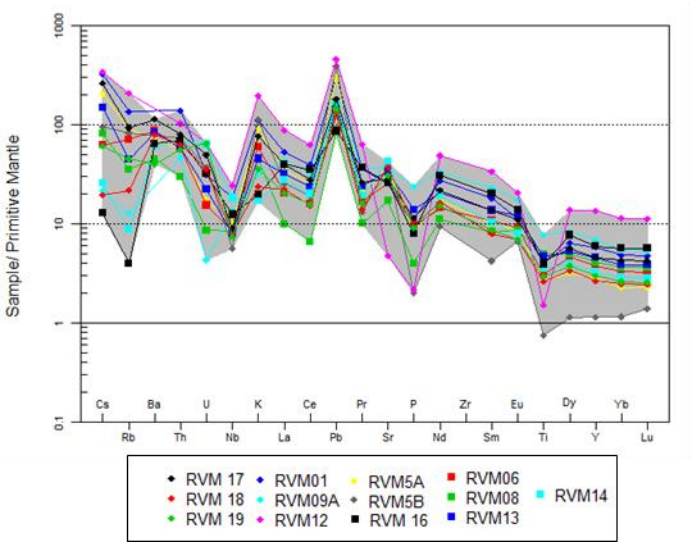

Fig. 12: Multi-element diagram of all samples normalized to primitive mantle values following Sun and McDonough (1989).

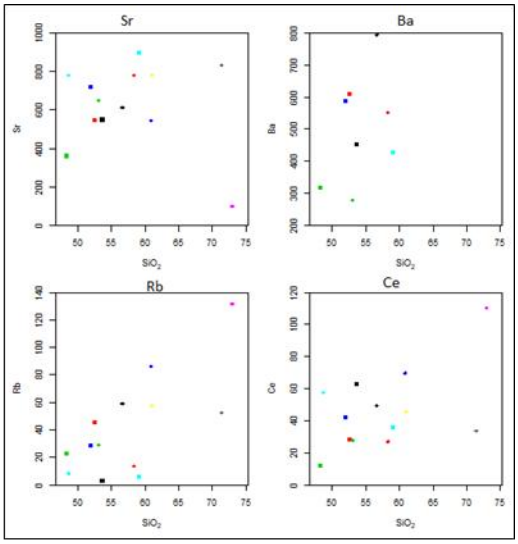

Fig. 13: Variation diagrams for all samples depicting SiO2 against LILE

After the REE normalized against chondrite values according to Anders and Grevesse 1989 (Fig.14), most of the projected samples show negative and gentle slope profiles showing enrichment in light rare earths (LREE) compared to heavy rare earths (HREE) with ratios LaN/ YbN = 2.57 - 20.85.

The ratios of LaN to SmN ranged from 0.93 to 5.91 (Table 2), all samples reveal a high concentration of LREE compared with HREE, with ratios greater than one (Rollinson H.,1993). Only RVM13 has a ratio less than one, indicating a depletion of LREE relative to HREE. It reflects the mineral fractionation or the alteration process. HREE values are intermediate to high and strontium Sr values are moderate.

RVM 05B -RVM09A- RVM17- RVM19 show no Europium anomalies compared to other REE with respectively (Eu/Eu*=1- 1.06- 1.09- 0.99).

RVM05A- RVM06 - RVM08- RVM12- RVM 13- RVM14- RVM16 show negative Europium anomalies compared to other REE with respectively (Eu/Eu*=0.92- 0.93- 0.76 -0.9 - 0.97 - 0.82- 0, 77) indicating its incorporation into the plagioclases (Zhou 2015) so the precursor magmas of these rocks underwent significant fractionation of plagioclase

RVM01-RVM18 show positive Europium anomalies compared with the other REE with respectively (Eu/Eu*= 1.12- 1.96) signifying an excess of plagioclase which indicate its fractionation so an early crystallization of plagioclase

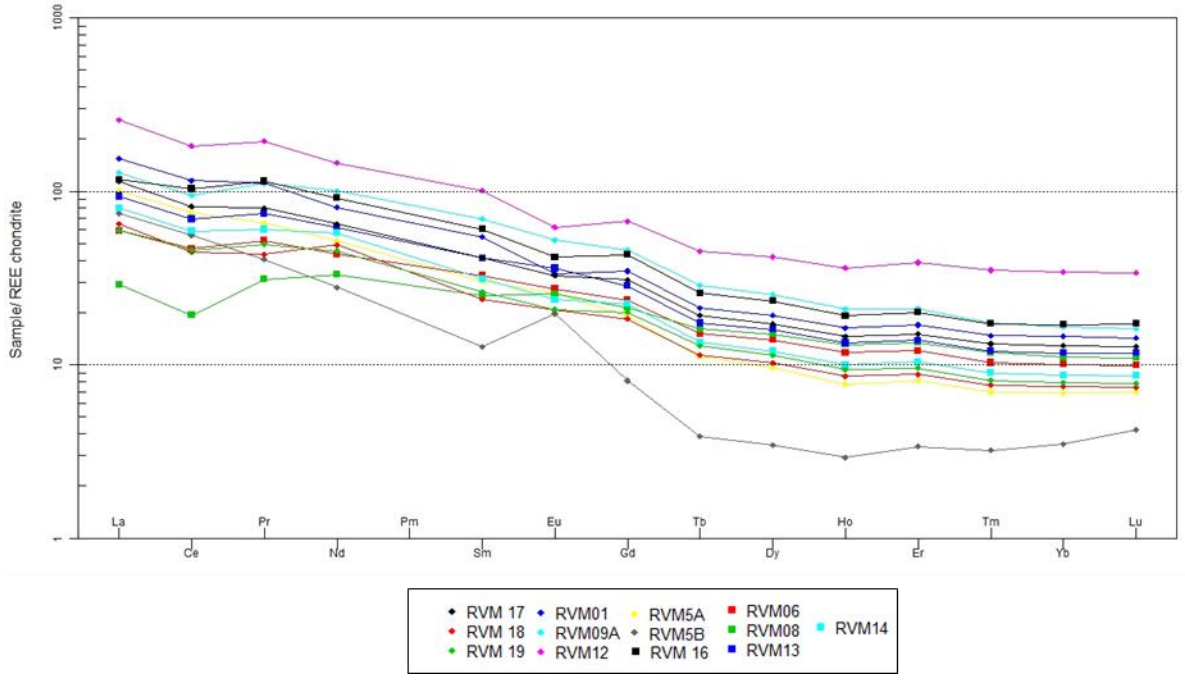

Fig. 14: Chondrite-normalised REE patterns for representative samples from the study area including the Manambato suite, Daraina Group and Milanoa Group according to Anders et Grevesse 1989

5. Discussions

5.1 Magmatic affinites and tectonic implication

As mentioned above, the igneous rocks in the study area exhibit a calc-alkaline affinity, characterized by high SiO_2, Na_2O, and CaO values. These results are consistent with previous studies conducted by Thomas,R.J, (2009), Tucker ,R et al., (2014), and Armistead et al., (2019). This calc-alkaline nature is further supported by the AFM ternary diagram from Irvine and Baragar (1971) (Fig.15).

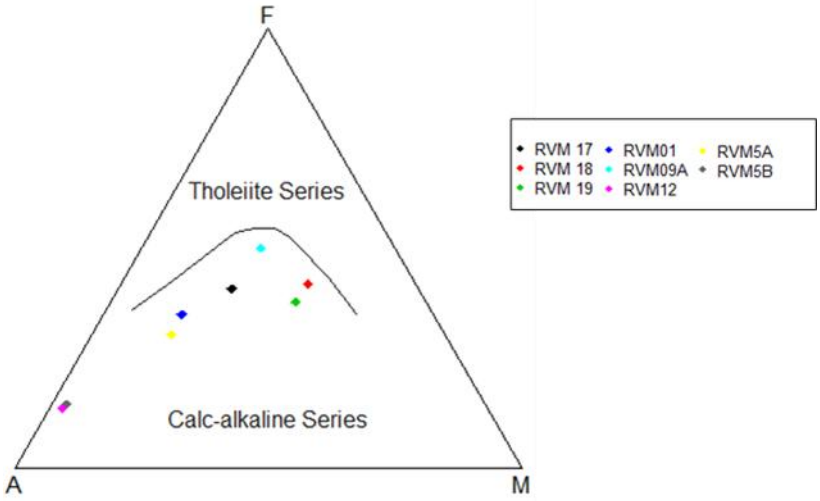

Fig. 15: discriminant diagrams AFM (FeOt vs. MgO vs. SiO_2) of plutonites from the study area based on Irvine and Baragar (1971):

Manambato suit (RVM 1- RVM05A – RVM05B - RVM 06- RVM17- RVM18- RVM19); Milanoa group (RVM12- RVM13- RVM14);

Daraina group (RVM08- RVM09A- RVM15)

The Shand index (1943), with (A/NK = 1.2- 2.4, A/ CNK = 0.8- 1.12) suggests crustal assimilation by the parent magmas, indicating that the protoliths are mafic to intermediate or infracrustal in origin. This geochemical signature is consistent with a Cordilleran tectonic setting and post-orogenic uplift (Beckinsale, 1979) (Figure 9b).

In the figure 10, the observed depletion of P_2O_5, MgO, CaO, and TiO_2, alongside a progressive increase in SiO_2, strongly supports the process of fractional crystallization. The reduction in P_2O_5, in particular, suggests the crystallization of apatite. The decline in TiO_2 content is likely due to the incorporation of rutile, ilmenite, or sphene into the crystalline phases or as accessory components within pyroxene or amphibole. Similarly, the depletion of FeO total indicates the fractionation of magnetite. The decreasing MgO content reflects the fractionation of olivine and clinopyroxene, while the reduction in CaO content suggests the crystallization of clinopyroxene and plagioclase. The Al_2O_3 trend, initially increasing and then decreasing, can be attributed to the fractionation of clinopyroxene followed by the crystallization of calcium-rich plagioclase. Meanwhile, the residual melt becomes progressively enriched in silica and alkalis, particularly K_2O, further confirming the fractional crystallization process. The Loss on Ignition (LOI) values of the metavolcanic samples indicate the presence of hydrated mineral phases such as amphibole or hydrothermal alteration minerals.

5.2 Tectonic discriminants

Using the La/10–Nb/8–Y/15 ternary diagram of Cabanis and Lecolle (1989), the granitoid rock samples are positioned within the orogenic compressive domain, specifically in the island arc and active margin regions, indicating a calc-alkaline nature (Fig.16a). In contrast, the basaltoid rocks are located above the mantle enrichment trend line (MORB-OIB) and fall within the continental arc field. This suggests the incorporation of crustal components into the mantle during subduction processes, as described by Fabio dos Santos Pereira et al. (2020) (Fig.16b).

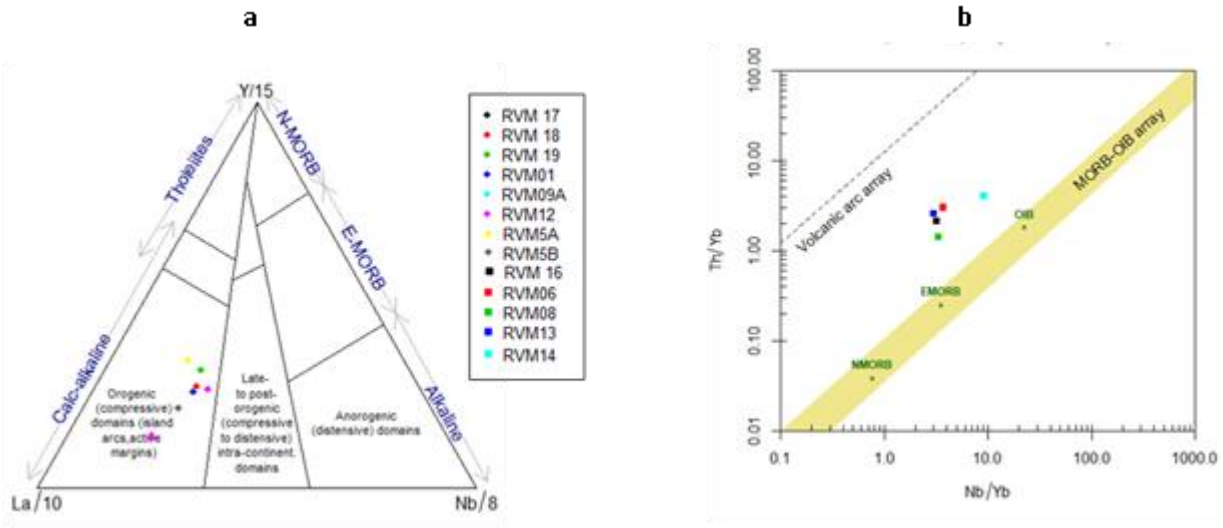

Fig. 16: (a) Granitoid rocks from the study area plotted on the La/10–Nb/8–Y/15 ternary diagram of Cabanis and Lecolle (1989). (b) Discrimination diagram between oceanic and non-oceanic basalts using the immobile trace element Th–Nb proxy diagram of Pearce (2008).

The significant depletion of High Field Strength Elements (HFSE) such as phosphorus (P), titanium (Ti), and niobium (Nb) suggests an orogenic sequence with a subduction-related signature (Michel Boily and Claude Dion., 2002). Additionally, the pronounced depletion of cerium (Ce) (Fig.14) is consistent with the incorporation of subducted sediments into the magma sources of the arc, as noted by Nina, B., et al. (2018). The enrichment in light rare earth elements (LREE) relative to heavy rare earth elements (HREE) further supports this subduction context.

Geotectonic classifications by Schandl and Gordon in 2002 align with the interpretation of an active continental margin setting, with magmas originating from subduction zones (Pearce, J., 2008; Catherine A. Stuart, 2022) (Fig. 17). Based on RRE signatures and magmatic affinities, we deduce that the magmas were generated above a subduction zone. The major and trace element compositions, along with REE ratios, indicate a source from a depleted mantle, with the involvement of hydrothermal fluids during magma formation.

The negative anomalies in Nb and Ti suggest the presence of titaniferous or amphibole phases in the mantle source. The low nickel (Ni), chromium (Cr), and cobalt (Co) contents in rocks such as RVM01, RVM05A, RVM05B, RVM09A, RVM12, RVM13, RVM17, RVM18, and RVM19 indicate that these rocks did not originate from partial melting of the deep mantle. Instead, they are consistent with magmatism from an active continental margin, where subduction zones contribute magmas enriched in amphibolite (Benali Hanafi, 2007).

These findings are further confirmed by the diagram of Smith, R. L., et al. (1999), which uses the Nb/La vs. La/Yb ratio to indicate that the source of most samples lies within the lithospheric mantle, except for RVM08 and RVM14, which show a mixed source of lithospheric and asthenospheric mantle. This suggests a weak assimilation of supra-crustal materials, with hydrothermal fluids playing a role during magma generation (Fig. 18). These post-eruptive hydrothermal alterations have led to the formation of hornblende, chlorite, and epidote in all geological formations, as described by Amarjargal Bars et al. (2018). The petrographical studies confirm the transformation of ferromagnesian minerals to the association of Quartz+ Chlorite +Amphibole+ opaque mineral (Fig7) and the transformation of the amphibole into a mineralogical association such as: epidote (pistachite) + chlorite + actinote + quartz (Razoeliarimalala, M., 2013)

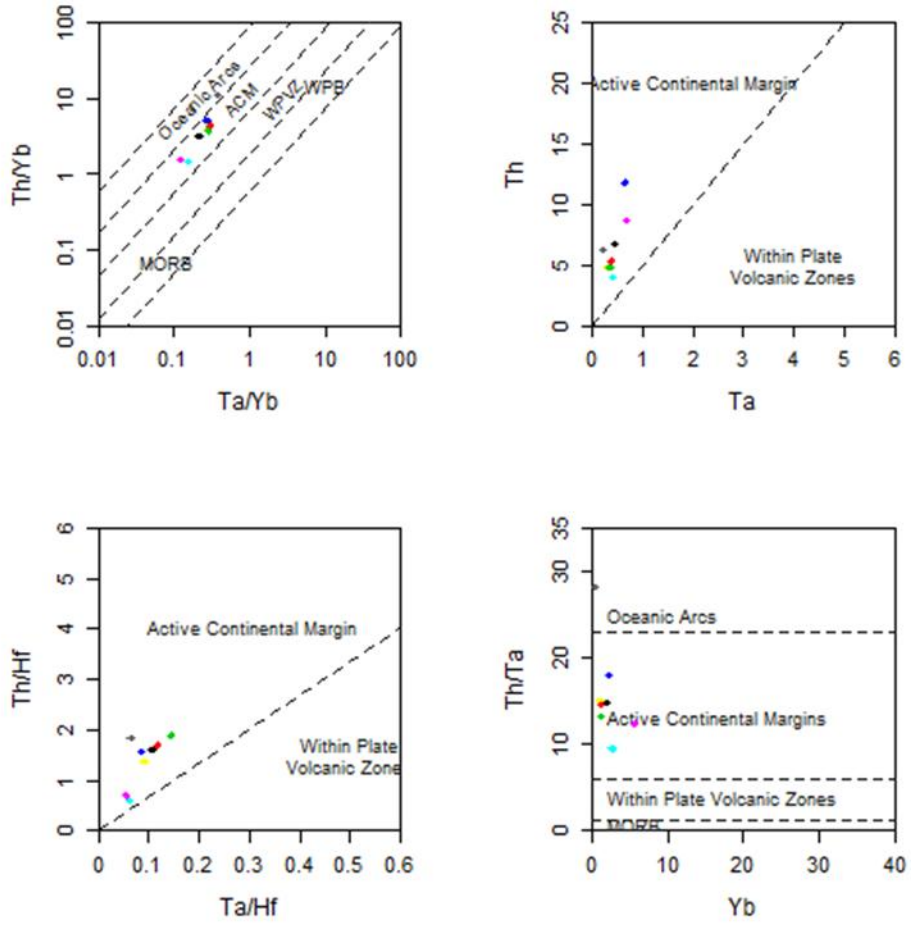

Fig 17: geotectonic classification of the plutonic rocks in the study area according to Schandl and Gordon (2002).

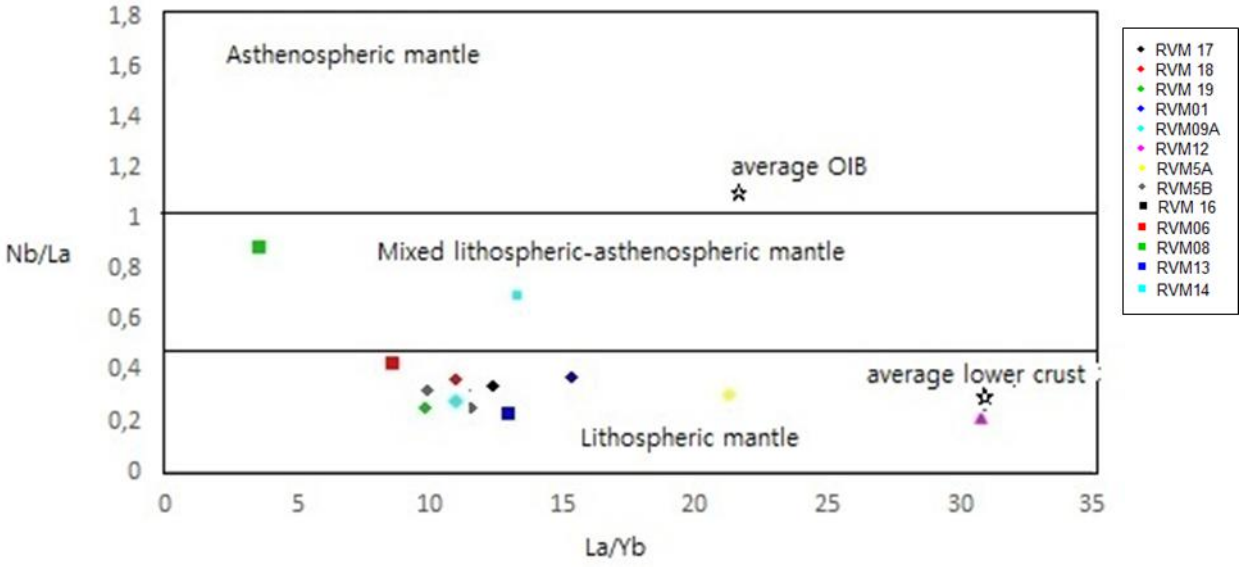

Fig. 18: Diagrams for identifying components of the mantle source of the study area. (a) Nb/La vs. La/Yb plot (modified after Smith et al., 1999; Karsli et al., 2014).

5. 3 Copper mineralization

Petrographic analysis reveals significant epidotization, chloritization and silicification of rocks, which occurs following the transformation of ilmenites, magnetites and ferromagnesian minerals due to the circulation of calcic hydrothermal fluids. This hydrothermal alteration particularly associated with the East African orogeny is responsible for the widespread copper mineralization of Mantsaborivaky Milanoa and across Africa (La Roche, H.D., 1958).

These alteration zones enriched in copper mineralization were concentrated along the brittle structures and remarkably at the intersection of N.60-80 E according to Bousteyak L. in 1974.

Based on the temperature of mineral paragenesis formations observed in thin sections, such as hematite, epidote, and crystalline quartz, these copper mineralizations are concentrated around 400°C, indicating a hydrothermal origin for the deposit (Brenon, P.1956; La Roche, H.D,1958).

In the figure 11, the positive correlations of Cu with oxides such as CaO, Al_2O_3, FeO total, MnO, TiO_2, MgO, and P_2O_5, as well as with trace elements including cobalt (Co), vanadium (V), lithium (Li), and zinc (Zn) suggest that geological environments enriched in these elements may be favorable for copper concentration. The observed correlations indicate that mineralogical, geochemical, and thermodynamic factors play a crucial role in the enrichment and deposition of copper in these settings. The negative correlations of Cu with oxides such as SiO_2, Na_2O, and K_2O, as well as with trace elements like lead (Pb), nickel (Ni), chromium (Cr), rubidium (Rb), cerium (Ce), and lanthanum (La) suggest that the accumulation of one set of elements occurs at the expense of the other, likely due to differences in mineral stability, magmatic differentiation, or hydrothermal alteration processes. These geochemical trends provide insight into the conditions that control copper mineralization and its association with specific rock-forming processes.

The correlations between copper and various oxides, as well as trace elements, suggest that copper mineralization in the Mantsaborivaky Milanoa area is predominantly concentrated in intermediate to mafic rocks, particularly in samples RVM08, RVM14, and RVM17. These mineralizations, along with

other metal sulfides, are concentrated in a reducing environment, consistent with a subduction-related context.

The study area displays tholeiitic and calc-alkaline magmatism, characterized by negative europium anomalies, a gently sloping REE pattern, and moderate strontium (Sr) values. These features are indicative of volcanogenic massive sulfide (VMS) deposits (Campbell, I.H., et al., 1982; Lesher, C. M., 1986; Vearncombe and Kerrich, R., 1999).

The Cu-Pb-Zn ternary diagram (Franklin et al., 1981) shows that the copper mineralization in the study area aligns with the Kuroko-type VMS, which is dominated by copper, zinc-copper, and zinc-lead-copper associations (Fig.19). Compared to other types of deposits, Kuroko-type VMS deposits are typically found in volcanic arc and back-arc basin settings, with lithologies composed mainly of volcaniclastic layers and terrigenous sedimentary rocks (Hannington, M.D.,2005) (Fig.20).

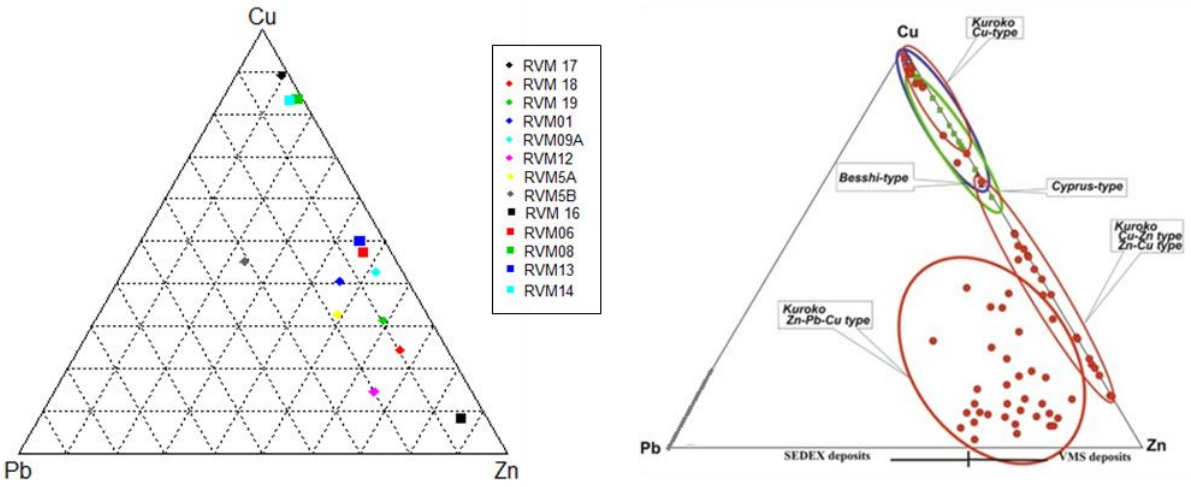

Fig. 19: Classification of volcanogenic Massive Sulfide deposits of Mantsaborivaky Milanoa according to Cu-Pb-Zn ternary diagram (Franklin et al., 1981)

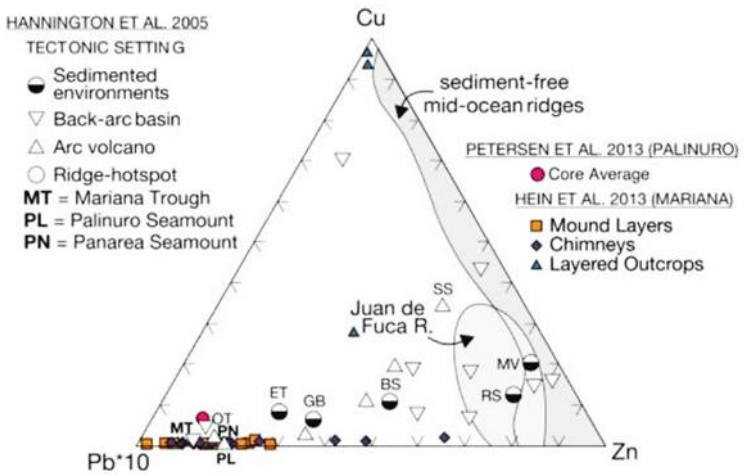

Fig. 20: Tectonic setting of some VMS deposits according to Hannington et al., 2005

6. Conclusion

In this study, we present petrographic descriptions and a new geochemical data from the Mantsaborivaky Milanoa area, providing insights into the typology of copper mineralization. The key conclusions are as follows:

(1) From petrographic studies, we conclude a deformation at high temperature environment, they thus deduce ancient mafic rocks underwent migmatitization following a higher-grade metamorphism. Thereafter, a significant fluid circulation enriched in calcium and potassium led to the alteration and transformation of ferromagnesians and feldspars. They induced the strong hydrothermal alteration consisting of: the propylitic alteration which is expressed by epidotization and chloritization; the sericitic alteration which is expressed by sericitization and the silicification.

(2) Hydrothermal alteration, being a process during East African Orogeny, is the source of the epidotization that accompanies copper mineralization in Mantsaborivaky Milanoa. Copper mineralization in the Mantsaborivaky Milanoa area is strongly associated with intermediate and, particularly, mafic rocks as amphibolo-epidotic rocks. The Manambato suite facilitated the mobilization of copper elements from ancient mafic eruptive rocks, expelling them to the surface. Descending fluid circulation transports these copper elements along brittle structures towards the magma chamber, where they impregnate deformed rocks. Hydrothermal fluids carrying copper mineralization then ascend freely along fractures.

(3) All geological formations of Mantsaborivaky Milanoa have a tholeiitic and alc-alkalic characteristics. The major elements analysis confirms the geological process mainly the fractional crystallization and contamination of the magma explaining the medium-K to high-K calcoalcaline composition. Plutonites present a granitic to gabbroic composition whereas volcanites show an andesitic to basaltic composition. They are all metaaluminous indicates a crustal assimilation in a cordilleran environment and post-, orogenic uplift.

(4) Mantsaborivaky Milanoa area is characterized by calc-alkaline magmatism associated with active continental margins, with magmas originating from subduction zones. These magmas contain amphibolite and are further influenced by partial melting of the lithospheric mantle, along with a mixture of lithospheric and asthenospheric mantle. Thus, the study area is situated in a back-arc basin.

(5) According to the classification of the volcanogenic massive sulphide, Mantsaborivaky Milanoa area is characterized by Kuroko-type volcanogenic massive sulfides, predominantly dominated by copper, zinc-copper, and zinc-lead-copper mineralization.in volcanic arc and back-arc basin contexts with a lithology generally consisting of volcaniclastic layers and terrigenous sedimentary rocks.

These findings contribute to the understanding of the geochemical processes driving copper mineralization in this region and highlight its potential for future exploration.

Acknowledgement

The authors wish to thank Wu Datian for his fundation and laboratory assistance. The authors are also grateful to two anonymous referees for their helpful comments and suggestions.

References

1. Armistead, S. E., Collins, A. S., Merdith, A. S., Payne, J. L., Cox, G. M., Foden, J. D., ... & De Waele, B. (2019). Evolving marginal terranes during Neoproterozoic supercontinent reorganization: Constraints from the Bemarivo Domain in northern Madagascar. Tectonics, 38(6), 2019-2035
2. Beckinsale, R. D. (1979). Granite magmatism in the tin belt of south-east Asia. In Origin of Granite Batholiths: Geochemical Evidence Based on a meeting of the Geochemistry Group of the Mineralogical Society (pp. 34-44). Boston, MA: Birkhäuser Boston
3. Bellot, N., Boyet, M., Doucelance, R., Bonnand, P., Savov, I. P., Plank, T., & Elliott, T. (2018). Origin of negative cerium anomalies in subduction-related volcanic samples: Constraints from Ce and Nd isotopes. Chemical Geology, 500, 46-63.
4. Benali, H. (2007). Les minéralisation associées aux roches magmatiques tertiaires du Nord de l'Algérie: typologie, pétrologie, cadre géodynamique, et implication métallogéniques (Doctoral dissertation).
5. BGS-USGS-GLW. (2008). Révision de la cartographie géologique et minière des zones minières des zones Nord, Centre, et Centre-Est de Madagascar (BGS Report CR/08/078). Keyworth, England: BGS.
6. Boily, M., & Dion, C. (2002). Geochemistry of boninite-type volcanic rocks in the Frotet-Evans greenstone belt, Opatica subprovince, Quebec: implications for the evolution of Archaean greenstone belts. Precambrian Research, 115(1-4), 349-371.
7. Bousteyak, L. (1974). Le socle cristallin dans l'extrême nord de Madagascar: Stratigraphie, étude pétrographique, essai de métallogénie (Doctoral dissertation, UER des sciences exactes et naturelles).

8. Brenon, P. (1952). Contribution à l'étude pétrographique et géologique des bassins de la Bemarivo et de la Fanambana (côte Nord-Est). Thèse de doctorat, Université de Nancy.
9. Brenon, P. (1954). Étude pétrographique et stratigraphique de la série de Milanoa. Laboratoire de Géologie et de Minéralogie de la Faculté des Sciences de Madagascar.
10. Brenon, P. (1956). Etude géologique et structurale des Régions cuprifères de Milanoa et d'Ambohijanahary. Bureau de Géologie, Archive, 1176.
11. Cabanis, B. (1989). Le diagramme La/10-Y/15-Nb/8: un outil pour la discrimination des séries volcaniques et la mise en évidence des processus de mélange et/ou de contamination crustale. Comptes rendus de l'Academie des sciences. Serie 2, 309, 2023-2029.
12. Campbell, I. H., Coad, P., Franklin, J. M., Gorton, M. P., Scott, S. D., Sowa, J., & Thurston, P. C. (1982). Rare earth elements in volcanic rocks associated with Cu–Zn massive sulphide mineralization: a preliminary report. Canadian Journal of Earth Sciences, 19(3), 619-623.
13. Collins, A. S., & Windley, B. F. (2002). The tectonic evolution of central and northern Madagascar and its place in the final assembly of Gondwana. The Journal of geology, 110(3), 325-339.
14. COMMISSION ECONOMIQUE POUR L'AFRIQUE (CEA). (1980) « Conférence régionale sur la mise en valeur et l'utilisation des ressources miné- rales en Afrique- Matières premières minérales en Afrique: Le cuivre » (pp. 63,68)
15. Cox K.G., Bell J.D., PankhurstR.J., (1979). The interpretation of igneous rock.George, Allen and Unwin, London.
16. Franklin,JM., Lydon,J.W and Sangster D.F., (1981) .Volcanic-associated massive sulfide deposits: Eonomic Geology.75th Anniversary volume,485-627
17. Hannington, M.D, Cornel,E.J, Sven, P.,(2005) . Sea- floor tectonics and Submarine hydrothermal systems.Society of Eonomic Geologists, Inc.Eonomic Geology 100th Anniversary Volume.111-141
18. Irvine, T. N., & Baragar, W. R. A. F. (1971). A guide to the chemical classification of the common volcanic rocks. Canadian journal of earth sciences, 8(5), 523-548.
19. Jöns, N., Schenk, V., Appel, P., & Razakamanana, T. (2005). P–T evolution of the Bemarivo Belt (northern Madagascar): the final assembly of Gondwana. Supercontinents and Earth Evolution, Geological Society of Australia, Abstracts, 81, 103R.
20. Jourde G., Rasamoelina, D., Ravelozon, S. A., & Razanakolona, J. 1967. Carte géologique de la République de Madagascar à 1/100 0000. Service géologique de Madagascar.
21. Jourde, G. (1968). Etude Geologique et prospection au 1/100000 des feuilles Betsiaka (V32), Antanambao (W32), Ampisikinana (X32), Milanoa (W33), Vohemar (X33), Andrafainkona (V34), Andravory (W34) et Antsirabe Nord (XY34). Bureau de Recherches Geologiques et Minieres, Antananarivo.
22. La Roche, H. D. (1958). Étude de la zone cuprifère de Vohémar (Archive 827). Bureau de Géologie.
23. La Roche, H. D. (1963). Etude geologique de l'extreme sud-est de Madagascar (Zone d'intensite metamorphique elevee), Metamorphisme des roches eruptives basiques et mineralisation cuprifere dans le nord-est de Madagascar (groupe de Daraina). Essai sur quelques problemes du metamorphisme des series silico-alumineuses (Doctoral dissertation, Nancy).
24. Lesher, C. M., Goodwin, A. M., Campbell, I. H., & Gorton, M. P. (1986). Trace-element geochemistry of ore-associated and barren, felsic metavolcanic rocks in the Superior Province, Canada. Canadian Journal of Earth Sciences, 23(2), 222-237.
25. Pearce, J. A. (2008). Geochemical fingerprinting of oceanic basalts with applications to ophiolite classification and the search for Archean oceanic crust. Lithos, 100(1-4), 14-48.
26. Razoeliarimalala M., 2013. Géologie du secteur de Milanoa et ses environs: Mise à jour sur la minéralisation cuprifère associée. Mémoire de DEA, Departement Sciences de la Terre, Université d'Antananarivo, Antananarivo.
27. Roig, J. Y., Tucker, R. D., Delor, C., Peters, S. G., & Théveniaut, H. (2012). Carte Géologique de la République de Madagascar à 1/1,000,000. Ministère des Mines, PGRM, Antananarivo, République de Madagascar, 1(1,000,000).
28. Stuart, C. A. (2022). Characterising VMS mineralisation at the Palaeoproterozoic Home of Bullion copper deposit, Aileron Province: in '. In Annual Geoscience Exploration Seminar (AGES) Proceedings, Alice Springs, Northern Territory 5–6 April 2022 (pp. 157-162).
29. Sun, S. S., & McDonough, W. F. ,1995. Chemical composition of the Earth's mantle. Geochimica et Cosmochimica Acta, 59(6), 1483-1495.
30. Thomas, R. J., De Waele, B., Schofield, D. I., Goodenough, K. M., Horstwood, M., Tucker, R., ... & Randriamananjara, T. (2009). Geological evolution of the Neoproterozoic Bemarivo belt, northern Madagascar. Precambrian Research, 172(3-4), 279-300.

31. Tucker, R. D., Ashwal, L. D., Hamilton, M. A., Torsvik, T. H., & Carter, L. M. (1999). Neoproterozoic silicic magmatism of northern Madagascar, Seychelles, and NW India: clues to Rodinia's assembly and dispersal. In Geological Society of America, Abstracts with Programs (Vol. 31, No. 7, p. 317).

32. Tucker, R. D., Roig, J. Y., Moine, B., Delor, C., & Peters, S. G. (2014). A geological synthesis of the Precambrian shield in Madagascar. Journal of African Earth Sciences, 94, 9-30. *

33. Vearncombe, S., & Kerrich, R. (1999). Geochemistry and geodynamic setting of volcanic and plutonic rocks associated with Early Archaean volcanogenic massive sulphide mineralization, Pilbara Craton. Precambrian Research, 98(3-4), 243-270.

34. Wilson,M., 1989.Igneous Petrogenesis, A Global Tectonic Approach. Unwin Hyman, London.

35. Zhou, J. L., Rasoamalala, V., Razoeliarimalala, M., Ralison, B., & Luo, Z. H. (2015). Age and geochemistry of Early Cambrian post-collisional granites from the Ambatondrazaka area in east-central Madagascar. Journal of African Earth Sciences, 106, 75-86.